

$\text{Sr}_2\text{Sb}_2\text{O}_7$: a novel earth abundant oxide thermoelectric

Luisa Herring Rodriguez^a, Kieran B. Spooner^a, Maud Einhorn^a and

David O. Scanlon^{a,b}

^a Department of Chemistry, University College London, 20 Gordon Street,
London, WC1H 0AJ, UK.

^b Thomas Young Centre, University College London, Gower Street, London
WC1E 6BT, UK

E-mail: d.scanlon@ucl.ac.uk

Convergence

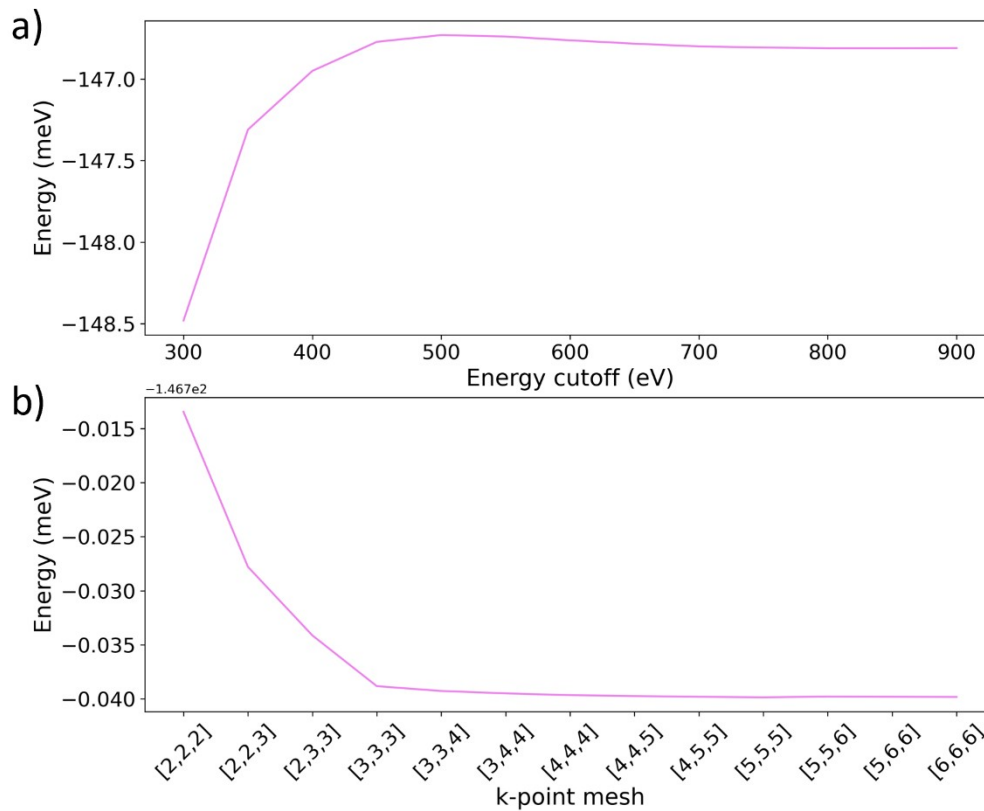


Fig. S1: The total VASP energies of Sr₂Sb₂O₇ against a) plane wave cut-off and b) k-point mesh. The values were converged to 10 meV atom⁻¹ at 500 eV and a k-point mesh of 3x3x3.

AMSET inputs

Table S1: The k-point meshes used in the density of states (DoS), the interpolated DoS used in AMSET, density functional perturbation theory (DFPT) and optics calculations for Sr₂Sb₂O₇. The high-frequency dielectric constant was calculated from the optics calculation, the ionic dielectric constant, elastic constant, piezoelectric constant (which in Sr₂Sb₂O₇ was 0) and polar optical phonon frequency were calculated from DFPT. The static dielectric constant is the sum of the high-frequency and ionic dielectric constants.

Calculation type	DoS	Zero-weighted DOS	DFPT	Optics
k-point mesh	7 × 8 × 8	11 × 11 × 11	3 × 3 × 3	6 × 6 × 6

$$\text{High frequency dielectric constant } \epsilon_0 = \begin{bmatrix} 2.88 & -0.02 & 0.01 \\ -0.02 & 2.88 & -0.01 \\ 0.01 & -0.01 & 2.90 \end{bmatrix}$$

$$\text{Static dielectric constant } \epsilon_0 = \begin{bmatrix} 13.48 & 0.55 & 1.62 \\ 0.53 & 13.51 & -1.57 \\ 1.63 & -1.56 & 12.84 \end{bmatrix}$$

$$\text{Elastic constant} = \begin{bmatrix} 267.9 & 72.7 & 100.8 & 0.5 & 1.1 & -7.5 \\ 72.7 & 267.9 & 100.8 & -1.4 & 7.5 & -1.3 \\ 100.8 & 100.8 & 240.9 & 0.9 & 5.5 & -5.7 \\ 0.5 & -1.4 & -0.9 & 69.0 & -0.2 & 0 \\ 1.1 & 7.5 & 5.5 & -0.2 & 97.8 & -0.1 \\ -7.5 & -1.3 & -5.7 & 0 & -0.1 & 97.8 \end{bmatrix}$$

Polar Optical phonon frequency (THz) = 10.00

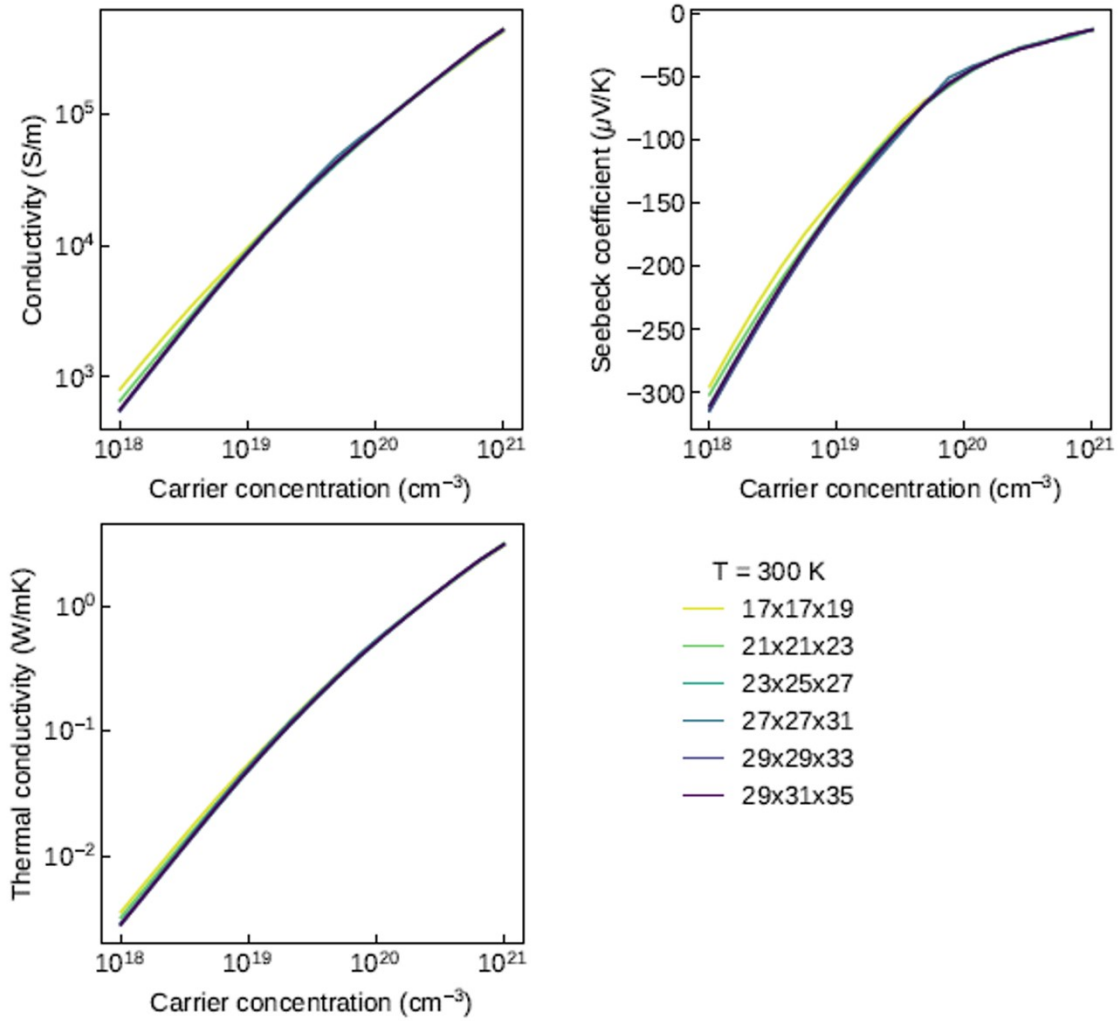


Fig. S2: Interpolation factor convergence at 300 K, with respect to the conductivity, Seebeck coefficient and thermal conductivity. It was converged at a factor of 15 ($23 \times 25 \times 27$).

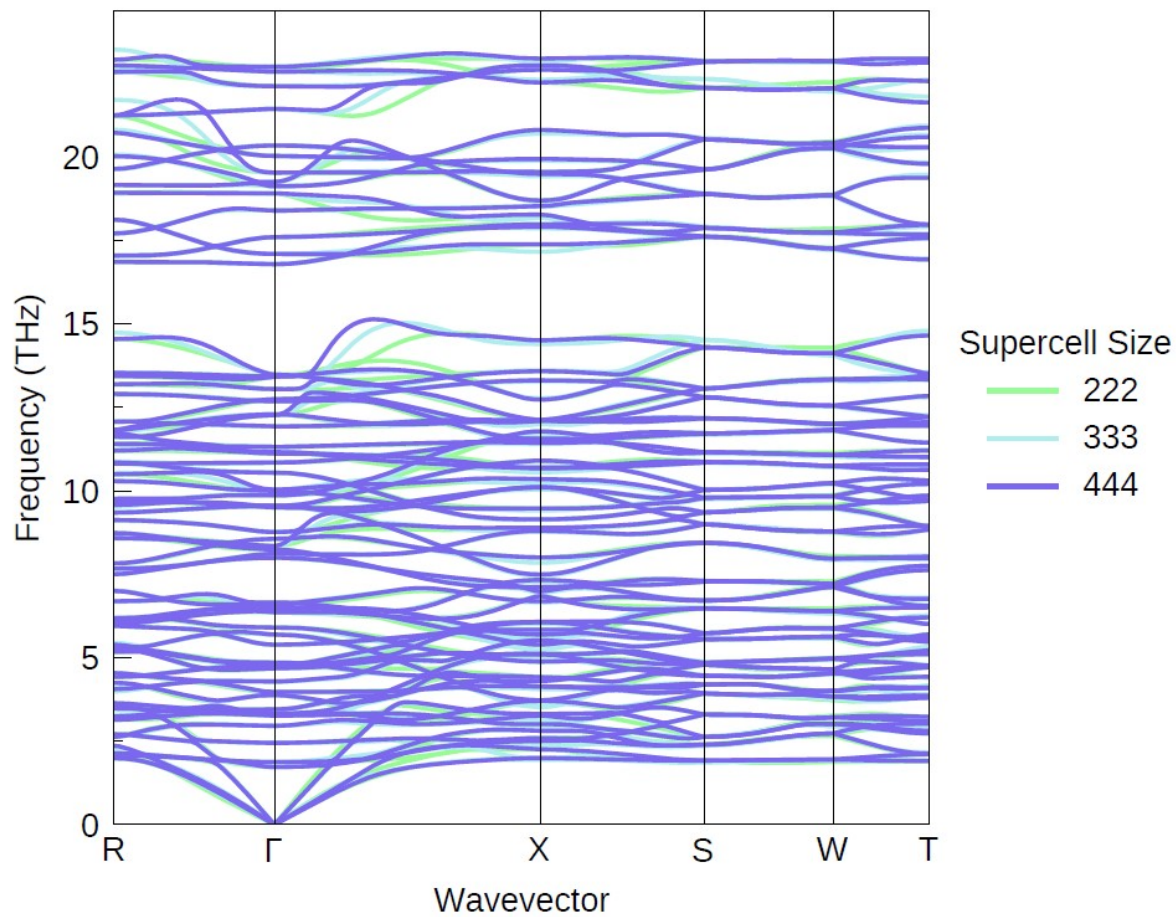


Fig. S3: Phonon supercell convergence. The key aspects of the phonon band structure are converged with the 2x2x2 supercell

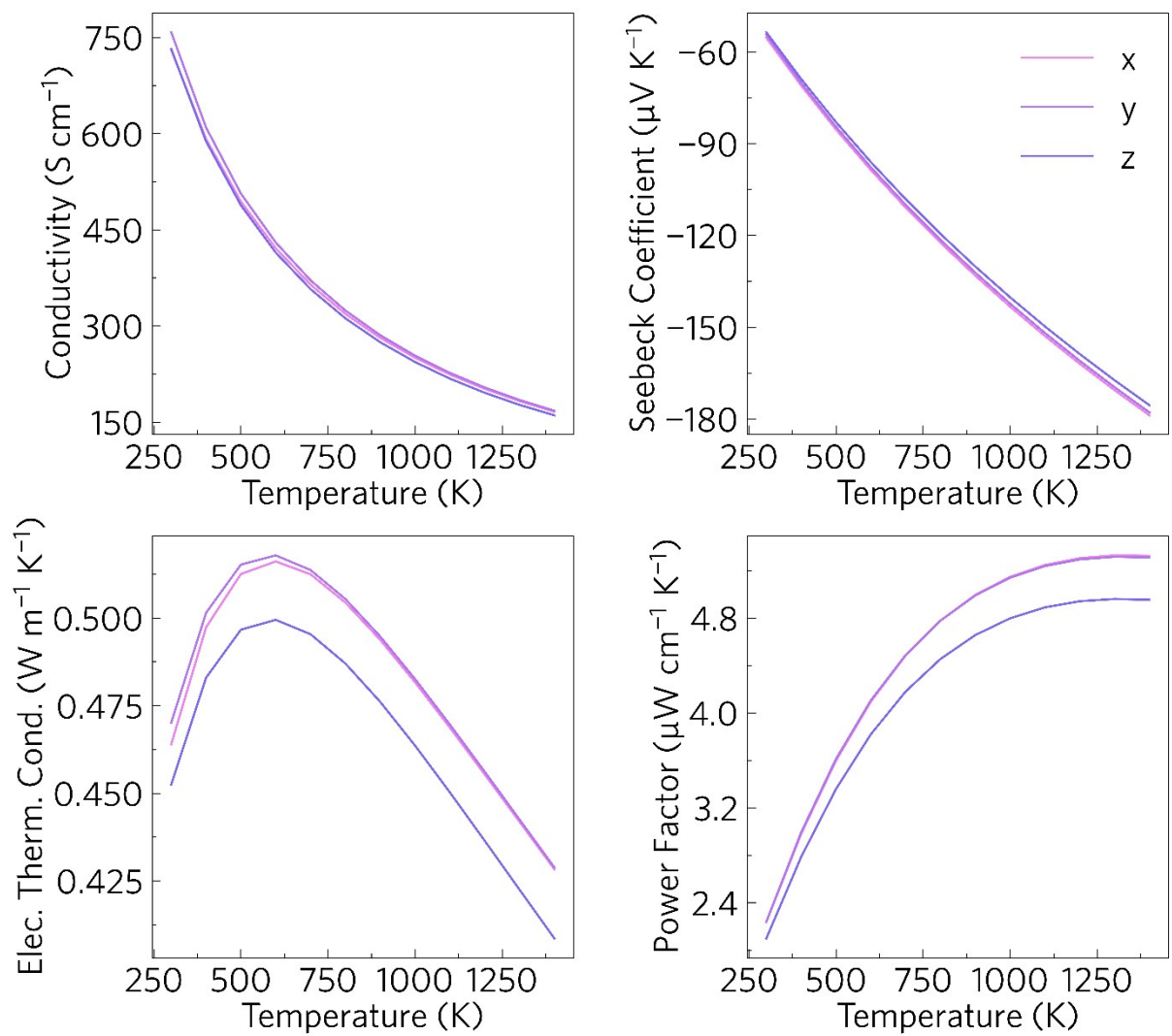


Fig. S4: Transport properties of $\text{Sr}_2\text{Sb}_2\text{O}_7$ split by direction.

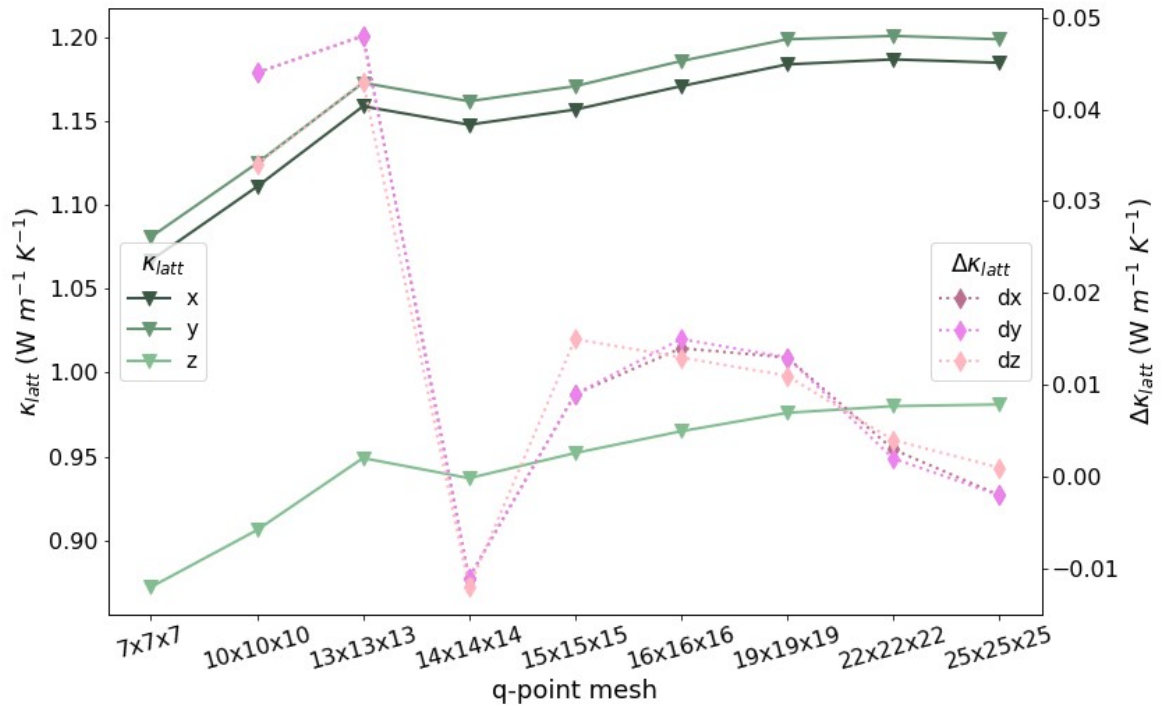


Fig. S5: Convergence of the lattice thermal conductivity at 1000 K against q-point mesh. The solid lines represent the lattice thermal conductivities in the x, y and z directions, and the dashed lines represent the change in lattice thermal conductivities in those directions. It converged to below $0.01 \text{ W m}^{-1} \text{ K}^{-1}$ in all directions at a mesh of $22 \times 22 \times 22$.

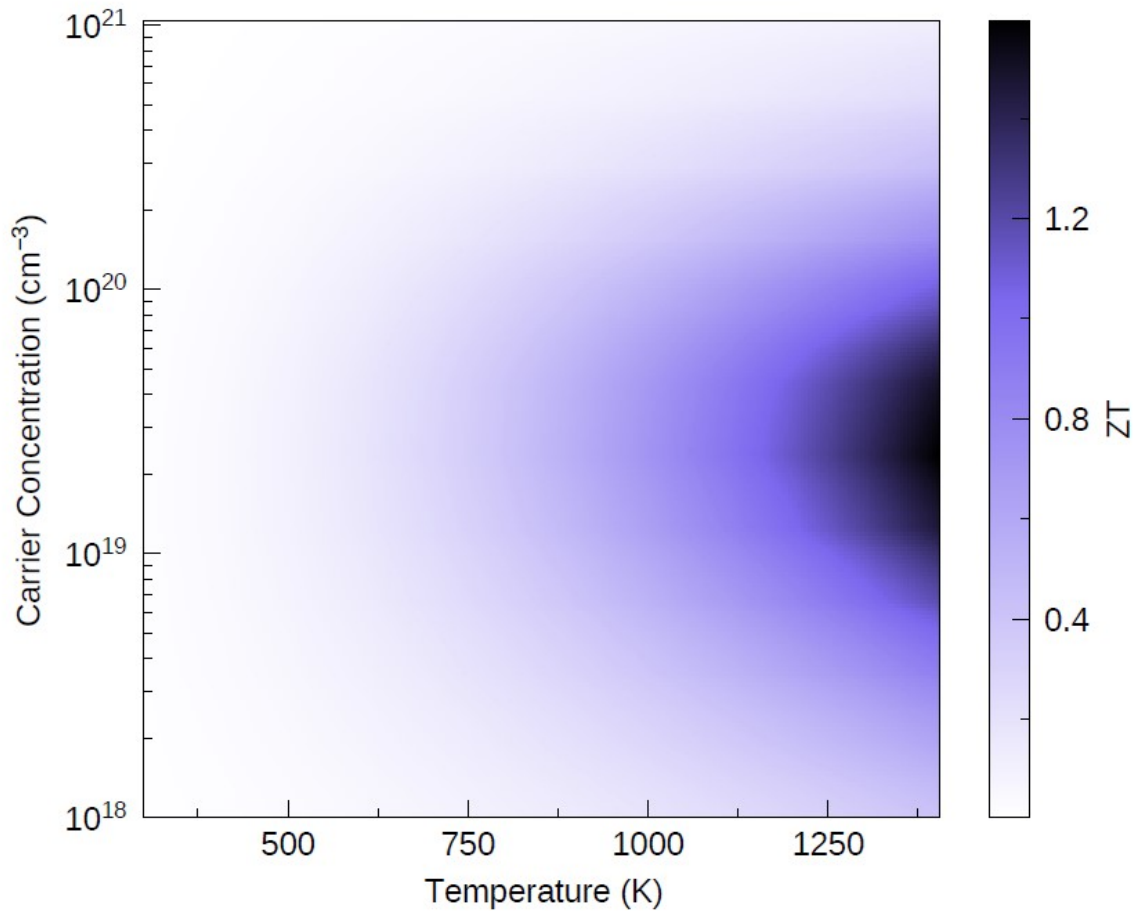


Fig. S6: ZT map calculated with the CTRA, with a maximum ZT of 1.6 at 1400K and a carrier concentration of $2 \times 10^{19} \text{ cm}^{-3}$

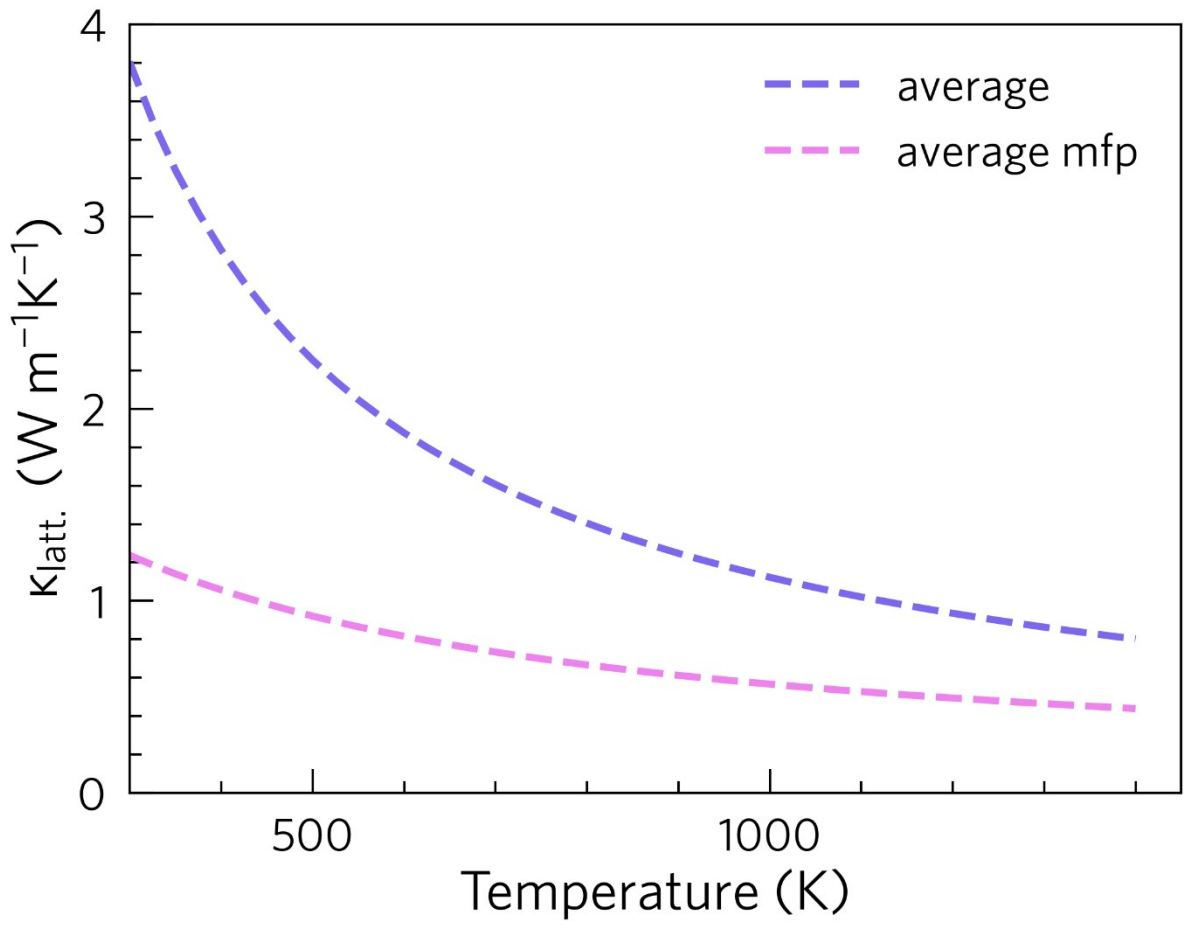


Fig. S7: Lattice thermal conductivity of $Sr_2Sb_2O_7$ calculated with and without nanostructuring to 10 nm.

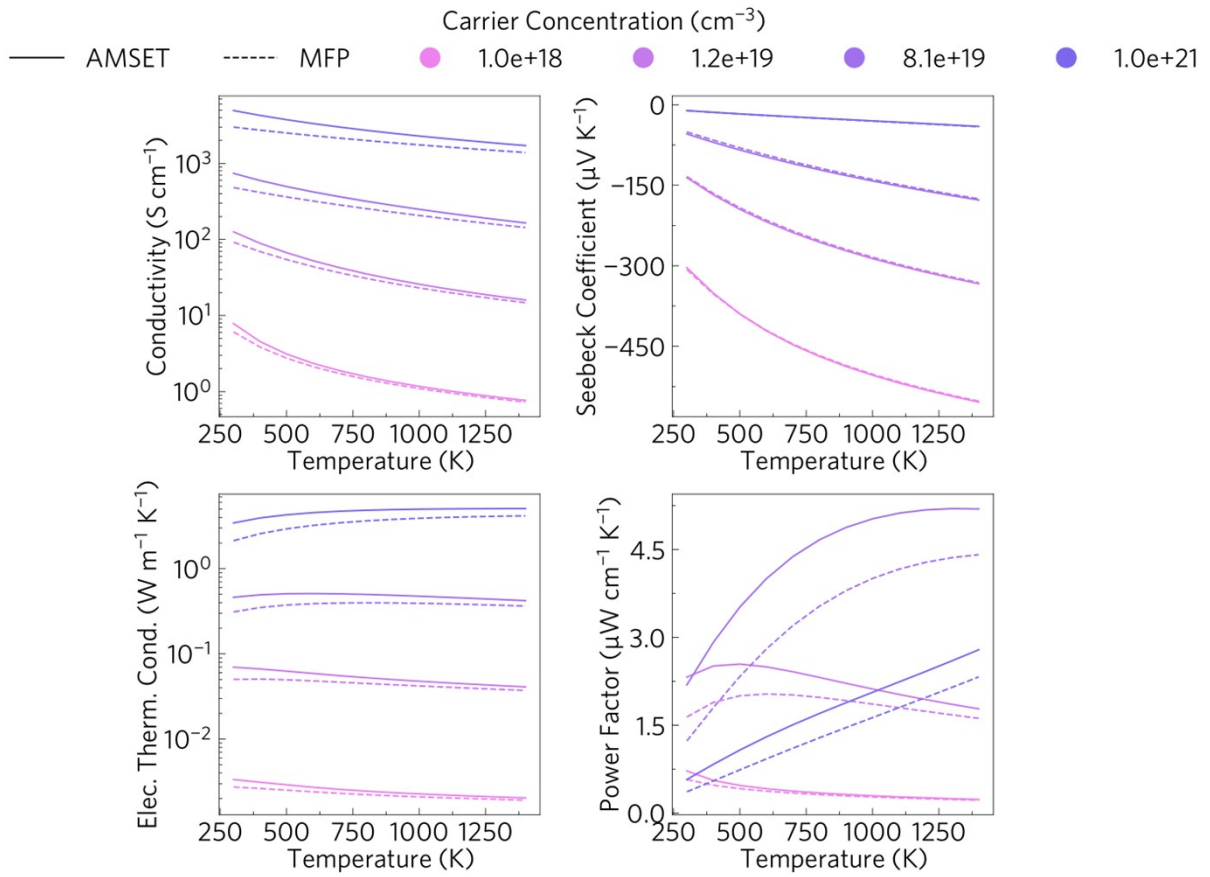


Fig. S8: Transport properties of $\text{Sr}_2\text{Sb}_2\text{O}_7$ with and without nanostructuring to 10 nm.